Preparation, DNA Binding, and *in Vitro* Cytotoxicity of a Pair of Enantiomeric Platinum(II) Complexes, [(*R*)- and (*S*)-3-Aminohexahydroazepine]dichloroplatinum(II). Crystal Structure of the *S* Enantiomer

Ronald R. Fenton,[1a] Warren J. Easdale,[1b] H. Meng Er,[1a] Shaun M. O'Mara,[1b] Mark J. McKeage,[1b] Pamela J. Russell,[1b] and Trevor W. Hambley*,[1a]

School of Chemistry, University of Sydney, NSW 2006, Oncology Research Centre, Prince of Wales Hospital, NSW 2031, Australia

Received November 18, 1996[⊗]

A pair of enantiomeric Pt(II) complexes, [Pt(*R*-ahaz)Cl_2] and [Pt(*S*-ahaz)Cl_2] (ahaz = 3-aminohexahydroazepine), has been investigated for their ability to bind enantioselectively to DNA. Improved synthetic procedures were developed for preparing both the ligands and the Pt complexes. The structure of the complex of the *S* enantiomer was determined by X-ray crystallographic methods. Crystals of [Pt(*S*-ahaz)Cl_2] are orthorhombic, space group $P2_12_12_1$, with $a = 6.917(1)$ Å, $b = 11.167(1)$ Å, $c = 12.373(2)$ Å, $Z = 4$, and the structure was refined to $R = 0.023$ (1505*F*). Molecular modeling techniques were used to investigate the role of steric interactions between the ligand and DNA in influencing the bifunctional binding of the two enantiomers, and it was found that the *S* enantiomer should bind more readily. The binding of the *S* enantiomer, to calf thymus DNA, was indeed found to be slightly greater than that for the *R* enantiomer though slightly less than that for *cis*-DDP. Assays of the proportion of monofunctional adducts showed that a substantially greater proportion of monofunctional adducts remained for the *R* enantiomer and cisplatin than for the *S* enantiomer. Each of the enantiomers was subjected to *in vitro* cytotoxicity assays using cultures of human bladder (BL13/0), lung and resistant lung (PC9 and PC9cisR), and prostate (DU145) cancer cells. The *R* enantiomer was found to be slightly more cytotoxic in the bladder cell line and may be less cytotoxic in the lung cell line but there were no significant differences in the resistant cell line nor in the prostate cell line. The two enantiomers were taken up equally by the bladder cancer cells.

Introduction

cis-DDP (*cis*-[Pt$(NH_3)_2Cl_2$]) and related compounds are believed to effect their anticancer activity by forming bifunctional adducts with DNA.[2−4] However, which of the bifunctional adducts is primarily responsible for the anticancer activity has not been unequivocally established. Our approach has been to design complexes to interact stereoselectivity with DNA, forming only a subset of the adducts and thereby acting as probes of the Pt/DNA interactions.[5−9] For example, we recently reported on the DNA binding of a compound designed to bind interstrand but not intrastrand.[9] The low activity of this compound *in vitro* provides evidence that the interstrand adduct is not the adduct primarily responsible for effecting cell death and indirect support for the notion that the intrastrand adduct is responsible.

We have also designed probes of the major intrastrand adducts which are to GpG and ApG sequences.[10] These adducts are chiral, and chiral Pt complexes therefore have the potential to react enantioselectively when forming such adducts. Some years ago Kidani and colleagues reported modest enantioselectivity for the pair [Pt(*R*,*R*-1,2-chxn)Cl_2] and [Pt(*S*,*S*-1,2-chxn)Cl_2] (1,2-chxn = 1,2-cyclohexanediamine).[11−13] Our first approach to the design of chiral probes, [Pt(*R*,*R*-eap)Cl_2] and [Pt(*S*,*S*-eap)Cl_2] (eap = *N*,*N*-diethyl-2,4-pentanediamine) met with only partial success with enantioselectivity based on *in vitro* cytotoxicity of less than 2:1.[10] We found that the pentanediamine framework was too flexible to impose the chirality at the nitrogen atoms that we sought and have now turned our attention to chiral complexes with more rigid ligand frameworks.

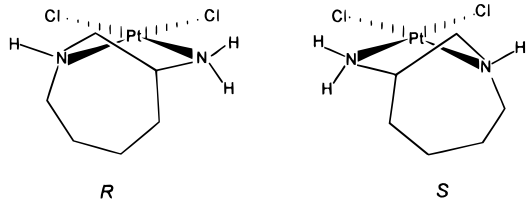

Figure 1. Schematic representation of the enantiomers of [Pt(ahaz)Cl_2].

In this context the ahaz ligand (shown in Figure 1) was considered to be ideal because it contains an endocyclic nitrogen atom and consequently has limited possibilities for conformational rearrangement once bound to a metal ion. The stereochemical properties of Cu complexes of ahaz have been studied extensively.[14−16] The complex [Pt(*L*-ahaz)Cl_2] has been reported to have antitumour activity,[17] but no details have been provided.

Experimental Section

Spectroscopy. ^1H and ^{13}C NMR spectra were recorded at 200.13 and 50.239 MHz, respectively, on a Bruker AC 200F spectrometer with solvents D_2O and $CDCl_3$ of 99.6% isotopic purity. Chemical shifts are reported in ppm (δ) relative to TMS or known solvent resonances used as internal calibrants. Infrared spectra were obtained on a Biorad FTS-40 spectrophotometer. Mass spectral data were recorded on Kratos MS902 mass spectrometer. Optical rotations were measured

⊗ Abstract published in *Advance ACS Abstracts,* March 1, 1997.

S0022-2623(96)00796-0 CCC: $14.00

at the sodium D line (589 nm) on an Optical Activity POLAAR 2001 polarimeter at ambient temperatures.

Preparations: (*R*)- and (*S*)-3-Aminohexahydroazepine. (*R*)-3-Aminohexahydroazepine was used as supplied by JPS Chimie, Bevaix, Switzerland. (*S*)-3-Aminohexahydroazepine was prepared by a modification of the method described by Saburi *et al.*[14] (*S*)-3-Aminohexahydroazepine (12.5 g, 98 mmol) was dissolved in sodium-dried THF (250 mL) and cooled to 0 °C in an ice bath. Freshly crushed $LiAlH_4$ (28.8 g) was added in small portions, and after all the $LiAlH_4$ had been added, the mixture was left to stand until it reached room temperature, whereupon the reaction was refluxed for 48 h. After being cooled to room temperature, the reaction mixture was transferred to a large conical flask and then further cooled in an ice bath. A solution of 57 mL of water in 100 mL of THF was then added very slowly to the reaction mixture, and the resultant mixture refluxed gently for 0.5 h. The mixed hydroxide solids were removed by suction filtration, and the filter cake was washed with boiling THF. The filter cake was then broken up, refluxed in 1,4-dioxane for 1 h, and then refiltered. All filtrates and washings were then combined, and the solvents were removed at reduced pressure to leave the crude ligand as a pale yellow oil. The crude product was then distilled at reduced pressure (ca 0.05 mmHg) to give a colorless oil in 60−65% yield.

[(*R*)- and (*S*)-3-Aminohexahydroazepine]dichloroplatinum(II). The complexes were first prepared by the Dhara method.[18] Briefly, $K_2[PtCl_4]$ (Aldrich, 0.50 g, 1.2 mmol) was dissolved in water (20 mL), and the solution was heated to 60 °C on a steam bath. Potassium iodide (0.83 g, 5 mmol) was added, and the solution was stirred for a few minutes. The ligand (1.2 mmol) was dissolved in the minimum volume of methanol and added to the $[PtI_4]^{2-}$ solution. The mixture was stirred for 1 h and allowed to stand overnight. The product was collected, washed with cold water, and transferred damp to a flask containing silver nitrate (0.41 g, 2.41 mmol). After 12 h of stirring in the absence of light, the silver iodide was removed. Aqueous sodium chloride (0.5 M) was added to the filtrate until no further silver chloride precipitated. Solid lithium chloride (1 g) was added, and the solutions were left to slowly evaporate over silica gel. The dark yellow-orange crystals were collected and washed with ice-cold water and ethanol. Yields: [Pt(*S*-ahaz)Cl_2] 0.32 g, 69%, [Pt(*R*-ahaz)Cl_2] 0.26 g, 57%. Anal. ($C_6H_{14}N_2Cl_2Pt$) C, 19.0; H, 3.7, N, 7.4. Found: [Pt(*R*-ahaz)Cl_2] C, 19.0; H, 3.7; N 7.4; [Pt(*S*-ahaz)Cl_2] C, 19.4; H, 3.7; N, 7.4. Infrared spectra (recorded on a BIO-RAD FTS spectrometer as a KBr pellet): ν_{max} (cm^{-1}) 3225 s, 3163 s, 3108 s, 2925 s, 2850 m, 1575 s, 1448 m, 1426 m, 1390 m, 1221 m, 1170 s, 1147 m, 1092 m, 1074 m, 1000 m, 960 m, 918 m, 836 m, 328 vs, 315 vs, 271 s.

[(*S*)-Aminohexahydroazepine]dichloroplatinum(II). The *S* enantiomer was subsequently prepared by an alternative method based on that described by Fanizzi *et al.*[19] [$Pt(DMSO)_2Cl_2$] was prepared by literature methods.[20] [$Pt(DMSO)_2Cl_2$] (0.42 g, 1.0 mmol) was suspended in methanol (40 mL), and the ligand (0.20 g, 1 mmol) in 20 mL of methanol was added. The resulting mixture was stirred until a clear pale-yellow solution resulted (∼1.5 h) and then stirred for a further 1.5 h. The solvent was removed on a rotary evaporator at 40 °C. The product was dissolved in water (20 mL), excess lithium chloride (0.5 g) was added, and the mixture was gently warmed on a steam bath until the volume was reduced to 10 mL. The fine pale yellow crystals that resulted were filtered off and washed with ice-cold water and ethanol. Further evaporation of the solution yielded additional crops of product. Total yield: 0.22 g, 57%. The IR spectrum obtained for each of the crops was identical to that obtained from the product synthesized via the $[PtI_4]^{2-}$ intermediate.

Crystallography: Structure Determination. For diffractometry a crystal was mounted on a glass fiber with cyanoacrylate resin. Lattice parameters at 21 °C were determined by least-squares fits to the setting parameters of 25 independent reflections, measured, and refined on an Enraf-Nonius CAD4F four-circle diffractometer employing graphite monochromated Mo Kα radiation. Intensity data were collected in the range $1\ \theta < 27.5°$. Data reduction and application of Lorentz, polarization, and analytical absorption corrections were carried out using the teXsan system.[21]

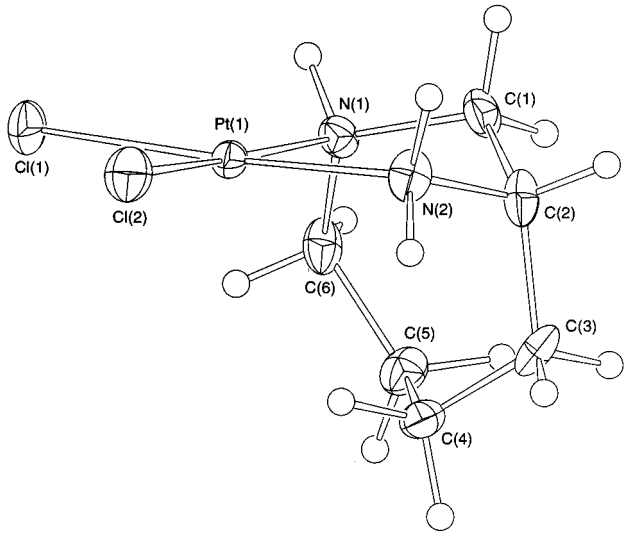

Figure 2. ORTEP plot of [Pt(*S*-ahaz)Cl_2] giving the crystallographic atom numbering; 30% probability ellipsoids are shown.

Table 1. Crystallographic Data[a]

chemical formula	$C_6H_{14}Cl_2N_2Pt$	fw	380.18
a, Å	6.917(1)	space group	$P2_12_12_1$
b, Å	11.167(1)	*T*, °C	21
c, Å	12.373(2)	*λ*, Å	0.71069
V, Å^3	955.7(2)	absorp coeff, cm^{-1}	152.38
Z	4	*R*	0.023
D_{calcd}, g cm^{-3}	2.642	R_w	0.024

[a] $R = \Sigma(||F_o| - |F_c||)/\Sigma|F_o|$, $R_w = (\Sigma w(|F_o| - |F_c|)^2/\Sigma wF_o^2)^{1/2}$.

Table 2. Bond Lengths (Å) for [Pt(*S*-ahaz)Cl_2]

Pt(1)−Cl(1)	2.320(2)	Pt(1)−Cl(2)	2.312(2)
Pt(1)−N(1)	2.044(6)	Pt(1)−N(2)	1.995(7)
N(1)−C(1)	1.48(1)	N(1)−C(6)	1.517(9)
N(2)−C(2)	1.51(1)	C(1)−C(2)	1.52(1)
C(2)−C(3)	1.54(1)	C(3)−C(4)	1.50(1)
C(4)−C(5)	1.52(1)	C(5)−C(6)	1.49(1)

Table 3. Bond Angles (deg) for [Pt(*S*-ahaz)Cl_2]

Cl(1)−Pt(1)−Cl(2)	94.52(9)	Cl(1)−Pt(1)−N(1)	91.6(2)
Cl(1)−Pt(1)−N(2)	174.9(2)	Cl(2)−Pt(1)−N(1)	172.9(2)
Cl(2)−Pt(1)−N(2)	89.6(2)	N(1)−Pt(1)−N(2)	84.1(3)
Pt(1)−N(1)−C(1)	108.6(5)	Pt(1)−N(1)−C(6)	116.7(5)
C(1)−N(1)−C(6)	112.4(6)	Pt(1)−N(2)−C(2)	112.1(5)
N(1)−C(1)−C(2)	110.6(7)	N(2)−C(2)−C(1)	105.4(7)
N(2)−C(2)−C(3)	109.9(7)	C(1)−C(2)−C(3)	114.9(7)
C(2)−C(3)−C(4)	116.9(7)	C(3)−C(4)−C(5)	113.7(7)
C(4)−C(5)−C(6)	116.4(6)	N(1)−C(6)−C(5)	116.5(7)

Structure Solution. The structure was solved by direct methods using SHELXS-86.[22] Hydrogen atoms were included at calculated sites with fixed isotropic thermal parameters. All other atoms were refined anisotropically. Full-matrix least-squares methods were used to refine an overall scale factor, positional, and thermal parameters. Neutral atom scattering factors were taken from Cromer and Waber.[23] Anomalous dispersion effects were included in F_c;[24] the values for $\Delta f'$ and $\Delta f''$ were those of Creagh and McAuley.[25] The values for the mass attenuation coefficients are those of Creagh and Hubbell.[26] All calculations were performed using the teXsan[21] crystallographic software package of Molecular Structure Corp., and plots were drawn using ORTEP.[27]

The atom numbering scheme is given in Figure 2, and bond lengths and angles are given in Tables 2 and 3. Observed and calculated structure factors, non-hydrogen atom positional and thermal parameters, hydrogen atom coordinates and thermal parameters, torsion angles, close nonbonded contacts, and

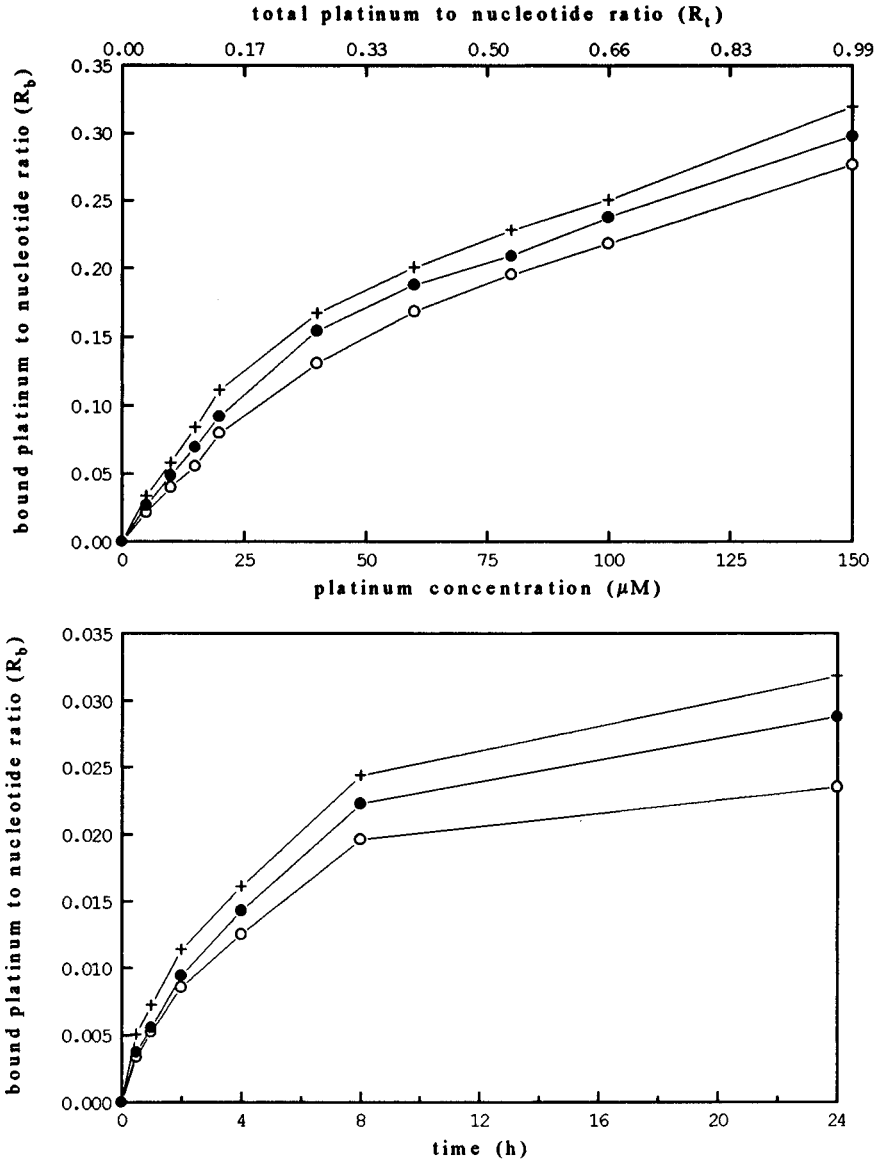

Figure 3. (a) Concentration dependent platinum-DNA binding curves for cisplatin (+), [Pt(*R*-ahaz)Cl_2] (○), and [Pt(*S*-ahaz)Cl_2] (●). (b) Time-dependent platinum DNA binding curves for cisplatin (+), [Pr(*R*-ahaz)Cl_2] (○), and [Pt(*S*-ahaz)Cl_2] (●) at an R_t value of 3.3×10^{-2}.

details of least-squares planes calculations (Tables S1−S7) are available as Supporting Information.

Molecular Modeling. DNA starting models (B-DNA, d(GpGpGpG*pG*pGpGpG):d(CpCpCpCpCpCpCpC)) were constructed using the HyperChem program.[28] A Pt atom was first bonded to the N7 atom of the 5′-guanine using HyperChem. A bifunctional adduct was then produced by reducing the distance between the Pt atom of the N7 of the 3′-guanine using constrained minimization in MOMEC-91.[29] Models of [Pt(*R*-ahaz)Cl_2] and [Pt(*S*-ahaz)Cl_2] were generated using HyperChem and were energy minimized using MOMEC-91 prior to docking with the bifunctionally platinated DNA in the appropriate orientations to produce the different isomers. These adducts were then energy minimized until the RMS shift was less than 0.05 Å. The force fields used for modeling the Pt complexes and the DNA were those described previously.[7]

DNA Binding. Concentration Dependence. Calf thymus DNA and Tris [tris(hydroxymethyl)aminomethane] were obtained from Sigma. The disodium salt of EDTA dihydrate was obtained from Merck. The 12−14 kDa dialysis membrane was purchased from Selby and was prepared by boiling in a solution containing 2% w/v sodium bicarbonate and 1 mM EDTA (pH 8.0) for 10 min, followed by rinsing thoroughly in distilled water and further boiling in 1 mM EDTA (pH 8.0) for 10 min. The membrane was cooled and stored in this solution at 4 °C. Dialysis was carried out using a BRL microdialysis system.

Graphite furnace atomic absorption spectroscopy (GFAAS) was performed on a Varian SpectrAA-20 absorption spectrometer equipped with a GTA-96 graphite tube atomizer and a PSC-56 autosampling system. UV absorbance was measured using a Hewlett-Packard diode array spectrometer.

The solutions of the platinum complexes were prepared immediately before being used by dissolving in TE buffer (10 mM Tris, 0.1 mM EDTA, pH 7.4 adjusted with 10 M HCl) with heating and sonication. These were filtered through 0.22 μm cellulose acetate filters (MFS).

Calf thymus DNA (25 μg) was reacted with the platinum complexes in TE buffer in a total volume of 500 μL. The final platinum concentrations ranged from 0 to 150 μM, which corresponded to *R* (molar ratio of platinum added to nucleotide) of 0 and 0.98, respectively. The reaction mixtures were incubated at 37 °C for 24 h and were then stopped by the addition of 56 μL of 2 M NaCl. Any unbound platinum species were removed by dialysis against 3 L of TE buffer at 4 °C. The concentration of DNA in each reaction mixture was determined by measuring the absrobance at 260 nm (ζ_{260} {DNA} = 6600 M^{-1} cm^{-1}). The bound platinum concentration was analyzed using GFAAS. The results are presented as plots of the R_b (molar ratio of platinum bound to nucleotide)

against the treated platinum concentrations in Figure 3a. Cisplatin was included in the assay for comparison.

Time Dependent Studies. The rates of platination of DNA by cisplatin and the enantiomers of [Pt(ahaz)Cl_2] were measured using a similar method to that described above. Briefly, calf thymus DNA (25 μg) was treated with 5 μM of the platinum complexes (which corresponded to an R_t value of 3.3×10^{-2}) in TE buffer. The mixtures were incubated at 37 °C for various time periods between 0 and 24 h, after which the reactions were terminated by the addition of NaCl (2 M, 56 μL). The samples were then dialyzed, and the R_b values shown in Figure 3b were determined as described above.

Rate of Monoadduct to Diadduct Conversion. The rate of monoadduct to diadduct conversion was measured using a method reported by Chaney *et al.*[30] Salmon sperm DNA (Sigma) (1 mg mL^{-1}, 2 mL) was incubated with freshly prepared platinum complexes (600 μM, 2 mL) in 25 mM NaCl, 0.2 mM EDTA, and 2 mM Tris-HCl, pH 7.4, at 37 °C for 30 min. The reactions were stopped by adding NaCl (2.5 M, 1 mL) and cooling to 4 °C. The samples were dialyzed against 1.5 L of high-salt TEN 7.4 buffer (10 mM Tris-HCl, 10 mM NaCl, 1 mM EDTA, pH 7.4, plus 0.5 M NaCl) at 4 °C (BRL Microdialysis System, Selby 12−14 Kdal dialysis membrane) for 2 h. The DNA samples were then precipitated with 4 mL of 2-propanol (Sigma, molecular biology grade) and centrifuged at 10 000 rpm at 4 °C, and the supernatants were decanted. These were resuspended in 2 mL of high-salt TEN 7.4 buffer and dialyzed against 1.5 L of 10 mM $NaClO_4$ at 4 °C for 2 h. The R_b values for the total platinum bound were measured as described above.

The above samples were divided into 200 μL aliquots and incubated at 37 °C for various time periods between 0 and 24 h. The level of monoadduct at each time point was determined by treatment with 20 μL of [^{14}C]thiourea (Sigma) (110 mM, 5.23 μCi $\mu$$mol^{-1}$, deionized over Bio-Rad AG501X8 resin) at 37 °C for 10 min. The reactions were stopped by adding 2 mL of cold 5% TCA (Sigma) and cooling on ice. The samples were then centrifuged at 10 000 rpm, and the supernatants were removed by aspiration.

The DNA pellets were redissolved in 200 μL of 0.1 M NaOH and then reprecipitated with 2 mL of cold 5% TCA. After the supernatants were removed by aspiration, the samples were dissolved in 200 μL of 0.1 M NaOH. Aqueous scintillant (Ultima Gold XR Scintillant) (1 mL) was added to each sample and mixed thoroughly, and the radioactivity of [^{14}C]thiourea bound to DNA was counted on a Wallac 1410 liquid scintillation counter. The background count was determined by an unplatinated DNA sample treated according to the procedure above.

Cytotoxicity Assays. The cell lines tested were human bladder tumor cells (UCRU BL 13/0),[31] lung cancer cells (PC9 and PC9cisR), and prostate cancer cells (DU145). (Note: PC9 is a cisplatin-sensitive cell line and its resistant variant, PC9cisR, has decreased intracellular drug accumulation and elevated cellular glutathione levels.[32,33])

The tumor cells were grown as a monolayer culture in RPMI 1640 culture medium, which was supplemented with 10% foetal calf serum (FCS), penicillin, and streptomycin. Exponentially growing cells were maintained in a humidified incubator at 37 °C in an atmosphere of 7.5% CO_2, 5% O_2, and 85% N_2 until 60−80% confluence. The pH of the culture medium was monitored with phenol red and maintained at 7.2. For subsequent drug assays, the cell monolayers were washed with Hanks buffered saline and treated with trypsin−EDTA to produce single cell suspensions. The cells were seeded at a concentration of 5000 cells per well in 100 μL of tissue culture medium in 96-well microtitre plates and incubated at 37 °C for 24 h.

The platinum complexes were dissolved in 0.9% (w/v) NaCl saline with gentle heating and sonication immediately prior to use and filtered through 0.22 μm cellulose acetate filters. The solutions were diluted with the tissue culture medium, and 100 μL portions were added into the wells so that the final concentrations in the wells ranged from 0 to 200 μM. After 96 h of drug exposure at 37 °C, the drug-containing medium was removed and the cells were washed with 200 μL of warm phosphate-buffered saline (PBS) followed by 200 μL of warm tissue culture medium. The viable cell concentrations were determined using either the MTT assay[34] or the SRB (Sulforhodamine B) assay.[35]

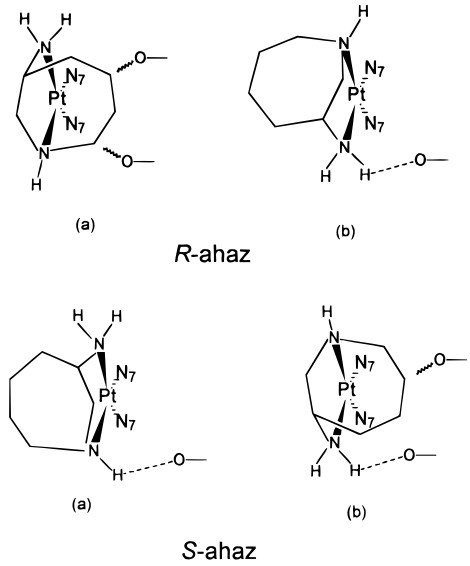

Figure 4. Schematic representation of the possible isomers formed when Pt(*R*-ahaz)$^{2+}$ and Pt(*S*-ahaz)$^{2+}$ bind to intrastrand GpG sequences of DNA.

MTT Assay. Cell viability was measured as the activity of the mitochondrial succinate dehydrogenase.[34] MTT (3-(4,5-dimethylthiazol-2-yl)-2,5-diphenyltetrazolium bromide) in FCS-free RPMI tissue culture medium (1 mg mL^{-1}, 200 μL) was added into each well, and the plates were incubated at 37 °C for 4 h. After centrifugation and removal of the MTT solution, the formazan formed at the bottom of the wells was solubilized with 2-propanol (200 μL). The optical density at 570 nm for the solution in each well was determined using a Dynatech MR 5000 plate reader.

SRB Assay. In this assay, sulforhodamine B was used to stain the basic amino acids.[35] After the cells in each well were fixed with 200 μL of ice-cold 10% trichloroacetic acid for 30 min at 4 °C, the plates were washed five times with tap water. The fixed cells were stained with 100 μL of 0.4% sulforhodamine B dissolved in 1% acetic acid for 15 min at room temperature. The stain was then removed, and the plates were washed five times with 1% acetic acid and left to air dry overnight. Tris (10 mM, 100 μL) was added to solubilize the dye in each well, and the absorbance at 570 nm was read using a Dynatech MR 5000 plate reader.

In both assays, the percentage of viable cells was calculated by comparing the absorbance of the platinum-treated cells to that of the untreated controls. Data were represented as the percentage of control versus the concentration of complex. The cell viability for each concentration was an average value for four or six replicates. The IR_{50} values for the drugs (the concentration required to kill 50% of the cell population) was determined from the dose−response curves.

Cellular Uptake of Platinum Complexes. The uptake of platinum complexes in human bladder tumour cells (BL13/0) was measured using a modification of a previously described method.[36] The cells were grown to 80% confluence in 60 × 15 mm tissue culture dishes. The freshly prepared solutions of platinum complexes in 0.9% (w/v) NaCl (filtered through sterile 0.22 μm cellulose acetate filters) were diluted to concentrations ranging from 0 to 100 μM with RPMI 1640 tissue culture medium supplemented with 10% FCS, penicillin, and streptomycin. Three tissue culture dishes were set up for each platinum concentration.

After the tissue culture medium was removed by aspiration, the monolayered cells in each tissue culture dish were treated with 5 mL of the drug solutions at 37 °C for 2 h. The drug-containing tissue culture medium was then removed, and the

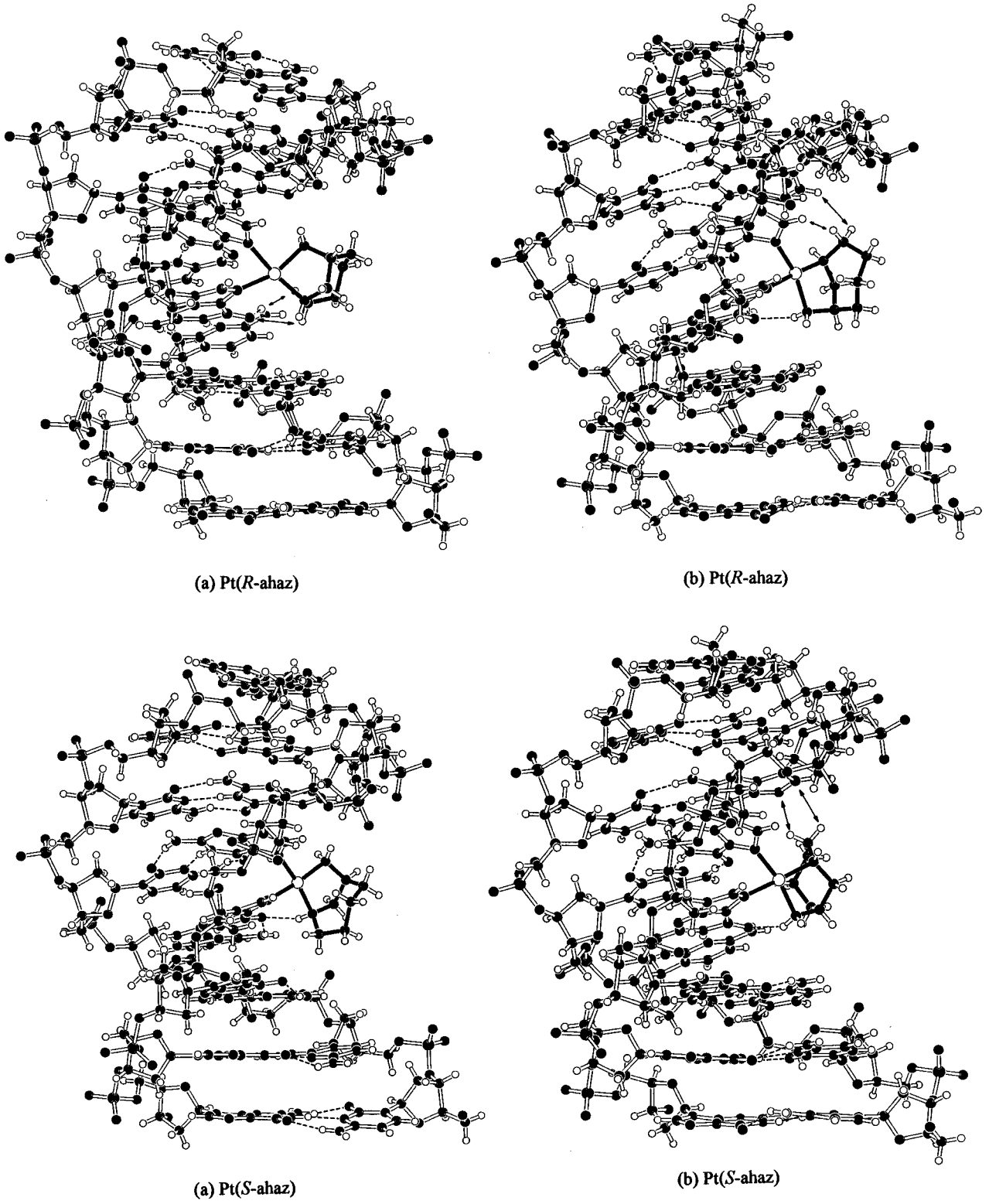

Figure 5. Energy-minimized models of the isomers formed by the binding of Pt(*R*-ahaz)$^{2+}$ and Pt(*S*-ahaz)$^{2+}$ to GpG sequences of DNA.

cells were washed three times with 25 mL of ice-cold PBS. The cells were scraped with 2 × 250 μL of ice-cold PBS, and the cell suspensions were lysed using a probe sonicator. The protein concentrations in the cell lysates were determined in duplicates using the Lowry assay,[37] and the platinum contents were analyzed using GFAAS.

To reduce the background absorption in the GFAAS measurements, the cell extracts were centrifuged for 5 min at 10 000 rpm. The supernatants were premixed with one volume of modifier (0.01% Triton X-100, 0.01% HNO_3 solution) in order to reduce the sample viscosity. The [K_2PtCl_4] standards were introduced with one volume of modifier into the graphite partition tube such that the final concentrations of the Pt standards ranged from 0.0 to 141.0 ppb. Three replicates were performed for the standards, and the samples were measured in duplicates. 2-Propanol (10%) was included into the sample dispenser cleaning fluid to prevent sample carry over.

Results and Discussion

Syntheses. Reduction of the caprolactam, (*S*)-3-aminohexahydroazepinone, with $LiAlH_4$ proved to be a

highly effective means of generating the ahaz ligand in high yield and purity. The complexes were initially synthesized via the $[PtI_4]^{2-}$ intermediate method first described by Dhara.[18] However, this is a relatively involved and time-consuming method and is less efficient when the ligand has secondary amine donor groups. In addition solubility problems were encountered when using the Dhara method. Therefore, we also refined the preparation of the *S* enantiomer using *cis*-$[Pt(DMSO)_2Cl_2]$ as a starting material. The method used is based on that described by Fanizzi *et al.*[19] and produces a [PtL(DMSO)Cl] intermediate. Care must be taken to avoid contamination by this intermediate in the final complex; however, we found that addition of excess lithium chloride yielded the pure $[PtLCl_2]$ complex in high yield. IR spectroscopy is a sensitive method for establishing that no DMSO remains in the final product. Reliable, high-yield synthesis of the complex sought were obtained in 3−4 h.

Description of the Structure. The structure consists of neutral [Pt(*S*-ahaz)Cl_2] molecules with only one weak H-bond between a H(amine) atom of one molecule and a chloro ligand of a symmetry related molecule [H(2)···Cl(2)^i 2.47 Å, $i = 0.5 + x, 0.5 - y, -z$]. There are more distant intramolecular contacts between the H(amine) atoms and the chloro ligands (H···Cl 2.93−3.14 Å). The situation is reversed in [Pt(*R*,*R*-eap)Cl_2] where the intramolecular H···Cl contacts are shorter (H···Cl 2.37−2.57 Å) than the closest of the intermolecular contacts (H···Cl 2.83−3.06 Å) because the H(amine) atoms lie close to the coordination plane.[10] We suggested that the close intramolecular contacts in [Pt(*R*,*R*-eap)Cl_2] stabilized the particular diastereomer observed.[10] Evidently, such interactions do not influence the conformational geometry in the present structure. The least-squares plane through the Pt atom and the four donor atoms shows deviations up to 0.11 Å. The deviations from planarity are unusual in that the four donor atoms lie on the same side of the Pt atom, with the deviations being greatest for the N atoms. The five-membered chelate ring adopts a slightly flattened, asymmetric conformation as indicated by the N−C−C−N torsion angle of −48.1(9)° and the unequal deivations of C(1) (0.50 Å) and C(2) (−0.16 Å) from the aforementioned least-squares plane. The seven-membered hexahydroazepine ring adopts a "skew chair" conformation in which four atoms, N(1), C(2), C(3), and C(6), define the approximately planar seat (deviations less than 0.12 Å), C(1) defines the back, and C(4) and C(5) lie skew to the plane. Similar conformations have been observed in other complexes of the ahaz ligand.[14−16] Somewhat surprisingly this conformation results in a close contact (2.72 Å) between the Pt atom and one of the H atoms bonded to C(4). Given the flexibility of the seven-membered ring (gross disorder has been observed in some structures), this contact might have been avoided if an alternative conformation had been adopted. This leads the question as to whether the contact represents a favorable (agostic) interaction or a weakly unfavorable nonbonded interaction. We have used molecular modeling techniques to investigate such interactions in this and related complexes and have concluded that the observations are consistent with the interaction being a weakly unfavorable nonbonded interaction if the van der Waals radius of Pt is in the range 1.6−1.8 Å.[38] The Pt−Cl bond lengths are not unusual, but the two Pt−N amine bond lengths differ significantly from one another. The Pt−N bond to the primary amine is at the short end of the range and that to the secondary amine is at the long end of the range.

Table 4. Minimized Strain Energies for the Isomers Formed When Pt(*R*-ahaz)$^{2+}$ and Pt(*S*-ahaz)$^{2+}$ Bind to Intrastrand GpG Sequences of DNA

isomer	strain energy (kJ mol^{-1})
R(a)	−2468
R(b)	−2476
S(a)	−2478
S(b)	−2483

Molecular Modeling. The GpG adducts formed when Pt(*R*-ahaz)$^{2+}$ and Pt(*S*-ahaz)$^{2+}$ bind to the starred site in the B-DNA sequences d(GpGpGpG*pG*pGpGpG): d(CpCpCpCpCpCpCpC) were modeled. Pt(*R*-ahaz)$^{2+}$ and Pt(*S*-ahaz)$^{2+}$ can bind to intrastrand GpG sequences of DNA in two ways: with the primary amine *cis* to the 5′ N7(guanine) atom (hereafter referred to as isomer a) or with the primary amine *trans* to this atom (isomer b). The four possibilities are shown schematically in Figure 4, and the energy minimized adducts are shown in Figure 5. The minimized strain energies are given in Table 4. The two isomers formed by the *R* enantiomer are less stable than those formed by the *S* enantiomer and the isomers with the primary amine *cis* to the 5′-guanine are less stable than the isomers where it is *cis* to the 3′-guanine. In the case of isomer *R*(*a*), no hydrogen bonding is possible between an amine proton and the 3′ O6 (guanine); instead there are close contacts (2.62, 2.65 Å) between H(carbon) atoms of the ahaz ring and this O atom. Isomer *R*(b) has the ahaz ring disposed away from the floor of the major groove, but the ring makes a close H···H contact (2.52 Å) with H8 of the 5′-guanine and a second longer contact (2.76 Å) to the H8 of the guanine on the 5′ side of the GpG pair. There is a hydrogen bond between the primary amine and O6 of the 3′-guanine (H(N)···O, 2.04 Å). Isomer *S*(a) also has the ahaz ring disposed away from the floor of the major groove, but because the bulk of the ring is oriented in the 3′ direction, no contact with H8 of the 5′-guanine or any other part of the DNA is observed. Indeed it is clear from Figure 5 that this orientation gives the least encumbered "fit" of the ahaz ring into the major groove. There is a hydrogen bond between the secondary amine and the O6 atom of the 3′-guanine. Isomer *S*(b) has a hydrogen bond between the primary amine and the 3′ O6 atom, but the ahaz ring is disposed toward the floor of the major groove. There are three close contacts between the ring and the DNA; 2.72 and 2.88 Å to the O6 and N7 atoms respectively of the 5′-guanine and 2.76 Å to the N7 of the guanine base at the 5′ side of the GpG pair. These observations are in general accord with the minimized strain energies, except that we might have expected isomer *S*(a) to be more stable than isomer *S*(b). The precision and accuracy of strain energies from calculations of molecules of this size is unknown; however, taken with the detailed observations, there is a clear indication that the *S* enantiomer should bind more readily than the *R*.

DNA Binding. The concentration and time dependent DNA binding assays reveal that, at all concentrations, cisplatin binds most readily, *S*-ahaz next, and

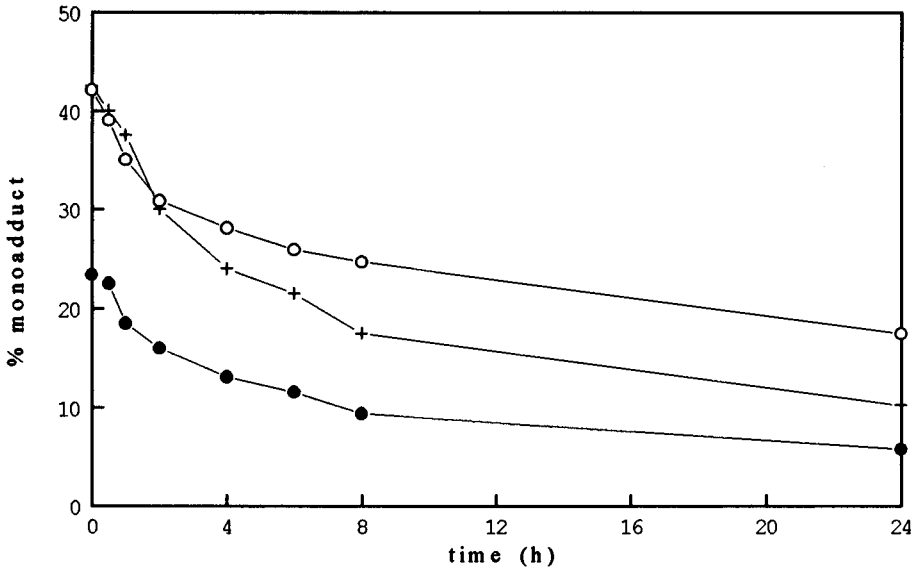

Figure 6. Monoadduct to diadduct conversion for cisplatin (+), [Pt(*R*-ahaz)Cl_2] (○), and [Pt(*S*-ahaz)Cl_2] (●).

R-ahaz least readily. Thus, these results accord with the predictions based on molecular mechanics modeling. That cisplatin binds more readily than either [Pt(*S*-ahaz)Cl_2] or [Pt(*R*-ahaz)Cl_2] is not unexpected, given its lesser steric bulk. What is surprising is that the difference is not greater; however, differences in the rates of hydrolysis that are dependent on the degree of substitution at the N donor atoms may play a role. Also, these assays are measuring total Pt binding and not discriminate between monofunctional and bifunctional binding.

Monoadduct to Diadduct Conversion. Studies were carried out to determine whether the enantiomers [Pt(ahaz)Cl_2] form different proportions of monofunctional adducts and to determine how rapidly these monofunctional adducts are converted to the bifunctional adducts. In these experiments, salmon-sperm DNA was incubated at 37 °C with the platinum complexes for 30 min. The DNA was precipitated with 2-propanol, and the ratio of the total bound platinum per nucleotide (R_b) was determined. The platinum-treated DNA was further incubated at 37 °C for 0−24 h to permit rearrangement of the monoadducts to diadducts. The monoadduct level at each time point was assessed by the incorporation of [^{14}C]thiourea under conditions that saturated the monofunctional adducts without causing reversal of DNA platination. The percentage of monoadduct was calculated as the ratio of the concentrations of monofunctionally bound platinum to total bound platinum.

At the platinum treatment concentration used in these experiments, the R_b values for cisplatin, [Pt(*R*-ahaz)Cl_2], and [Pt(*S*-ahaz)Cl_2] are 4.0×10^{-2}, 3.0×10^{-2}, and 3.3×10^{-2}, respectively. The monoadduct levels over a 24 h time period for these complexes are displayed in Figure 6.

At the first timepoint (30 min after the initial reaction), similar numbers of monofunctional adducts remain for cisplatin and [Pt(*R*-ahaz)Cl_2] but only half this number remain for [Pt(*S*-ahaz)Cl_2]. This suggests that a large proportion of the bound [Pt(*S*-ahaz)Cl_2] has rapidly formed bifunctional adducts. The more rapid closure to the bifunctional adduct by the *S* enantiomer is in accord with the molecular models that show that both orientations of the *R* enantiomer lead to clashes with the DNA but one of the orientations of the *S* enantiomer does not lead to any clashes. The monofunctional adducts formed by [Pt(*S*-ahaz)Cl_2] and [Pt(*R*-ahaz)Cl_2] then disappear at similar rates and eventually level off with a larger proportion of monofunctional adducts remaining for the *R* enantiomer. A similar difference in the proportions of monofunctional adducts for [Pt(*S*-ahaz)Cl_2] and [Pt(*R*-ahaz)Cl_2] has emerged from preliminary studies of the adduct profiles using enzymatic digestion and HPLC analysis.[39]

A more rapid initial drop off is observed for cisplatin, but after 24 h there remains a greater proportion of monofunctional adducts than is observed for [Pt(*S*-ahaz)Cl_2]. Interpretation of these results is complicated by the likelihood that two processes are taking place: closure to bifunctional adducts where initial attack was at a GpG or ApG site and migration from isolated G sites to GpG or ApG sites followed by closure. If this is the case, then differences between the three compounds will result from both differences in reaction rates *trans* to NH_3 and primary or secondary amines and differences in steric bulk.

Table 5. Cytotoxicity (IC_{50}) Values (μm) Determined in Human Tumor Cell Lines[a]

platinum complexes	IC_{50} (μM)			
	UCRU BL13/0	PC9	PC9cisR	DU145
	MTT Assay			
cisplatin	1.9(5)	1.4(2)	11.7(31)	1.8(8)
[Pt(*R*-ahaz)Cl_2]	1.3(2)	5.9(1)	16.0(10)	2.9(1)
[Pt(*S*-ahaz)Cl_2]	2.0(2)	3.0(4)	15.5(13)	3.4(3)
	SRB Assay			
cisplatin	9.5(18)	5.0(5)	>17.5	1.0(2)
[Pt(*R*-ahaz)Cl_2]	7.2(4)	11.0(15)	27.3(35)	3.3(2)
[Pt(*S*-ahaz)Cl_2]	12.3(7)	11.7(9)	25.0(15)	3.7(3)

[a] Numbers in parentheses are standard errors in units of the last significant figure quoted.

Cytotoxicity Studies. Both enantiomers of [Pt(ahaz)Cl_2] show cytotoxic activity comparable with that of cisplatin toward cultures of human bladder tumor cells (Table 5). The *R* enantiomer is more active than the *S* enantiomer, by factors of 1.5 and 1.7 according to the MTT and SRB assays, respectively. In the PC9, PC9cisR, and DU145 cell lines, both enantiomers are

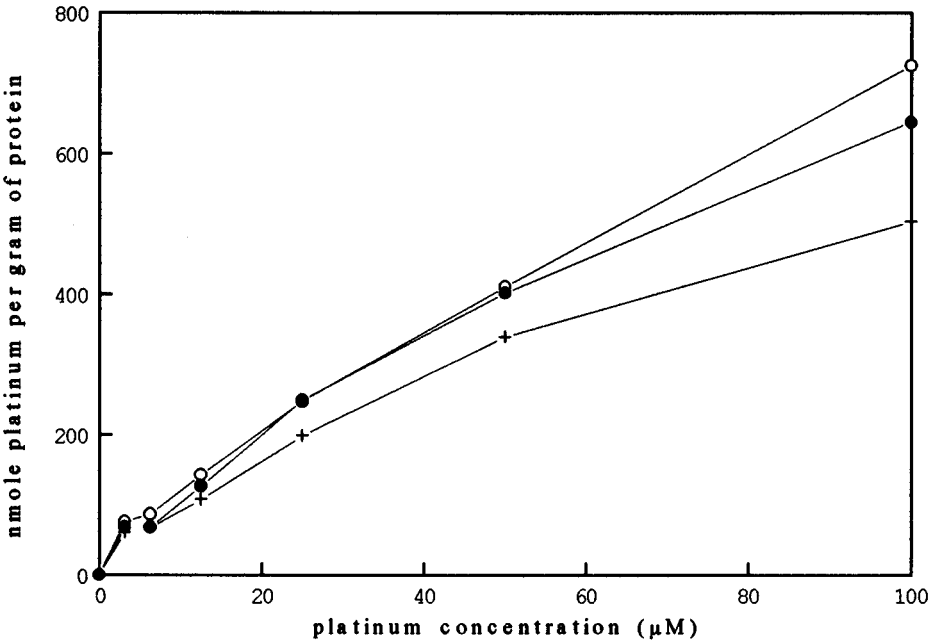

Figure 7. Uptake in BL13/0 cells for cisplatin (+), [Pt(*R*-ahaz)Cl_2] (○), and [Pt(*S*-ahaz)Cl_2] (●).

less active than cisplatin although they are not fully cross resistant in the PC9cisR cell line and there is no clear enantioselectivity.

Cellular Uptake of Platinum Complexes. In order to establish whether the difference between the *in vitro* cytotoxic activities of the enantiomers of [Pt(ahaz)Cl_2] in the BL 13/0 cell line is caused by the differences in the efficiency of transportation across the cell membrane, cellular uptake studies of these complexes in the human bladder cells were carried out and the results are shown in Figure 7.

Higher amounts of the enantiomeric [Pt(ahaz)Cl_2] complexes entered the cells than cisplatin over the entire platinum treatment concentration range. This can be explained by the increased lipophilicity of these complexes due to the presence of the ahaz ligand. The cellular uptake curves reveal that the *R* enantiomer was transported across the cell membrane at a slightly higher level than the *S* enantiomer at all platinum treatment concentrations. It is unlikely that this marginal difference was a significant factor in the difference observed in the *in vitro* cytotoxic activities of these enantiomers in the human bladder cancer cell line.

Conclusions

The two enantiomers of [Pt(ahaz)Cl_2] were investigated to establish whether they demonstrated any enantioselectivity in their DNA binding and cytotoxic action. On the basis of computer-generated models we predicted that the *S* enantiomer should bind more readily to DNA than the *R* enantiomer, and this was borne out by measurements of binding to calf thymus DNA. Also, we found that closure of monofunctional adducts occurred more rapidly for the *S* enantiomer, again in accord with the molecular models. Modest but reproducible enantioselective differences in cytotoxicity were observed in cultures of human bladder cancer cells, but surprisingly, it was the *R* enantiomer that was found to be the more active. In lung and prostate cell lines, no reproducible differences were observed. Since the differences in cytotoxicity do not correlate with simple measurements of DNA binding or the rate of closure of monofunctional adducts, we need to consider other possibilities. Cellular uptake does differ slightly for the two enantiomers, but not at a level that is likely to contribute to the difference in activities. Enantioselective differences in cytotoxicity might arise from differences in deactivation by intracellular components, interactions with DNA, or repair of DNA adducts. Alternatively, the profile of adducts produced on DNA binding or the bending induced in the DNA by each enantiomer could be important. Experiments are underway to investigate the role of each of these possible factors.

Acknowledgment. The support of the Sydney University Cancer Research Fund, the University of Sydney Research Grants Scheme, and the Australian Research Council is gratefully acknowledged.

Supporting Information Available: Tables of crystal data, positional and thermal parameters, bond lengths and angles, torsion angles, least-squares planes, and nonbonded distances (8 pages); observed and calculated structure factors (6 pages). Ordering information is given on any current masthead.

References

(1) (a) School of Chemistry, University of Sydney. (b) Oncology Research Centre, Prince of Wales Hospital.
(2) Pinto, A. L.; Lippard, S. J. Binding of the antitumor drug *cis*-diamminedichloroplatinum(II) (cisplatin) to DNA. *Biochem. Biophys. Acta* **1985**, *780*, 167−180.
(3) van der Veer, J. L.; Reedijk, J. Investigating antitumour drug mechanisms. *Chem. Br.* **1988**, *24*, 775−780.
(4) Sheibani, N.; Jennerwein, M. M.; Eastman, A. DNA repair in cells sensitive and resistant to *cis*-diamminedichloroplatinum-(II): Host cell reactivation of damaged plasmid DNA. *Biochemistry* **1989**, *28*, 3120−3124.
(5) Hambley, T. W. What can be learnt from computer generated models of interactions between DNA and Pt(II) based anti-cancer drugs? *Comments Inorg. Chem.* **1992**, *14*, 1−26.
(6) Hambley, T. W. Why does cisplatin bind to ApG but not GpA sequences of DNA? A molecular mechanics analysis. *Chem. Commun.* **1988**, 221−223.
(7) Hambley, T. W. A molecular mechanics analysis of the stereochemical factors influencing monofunctional and bifunctional binding of *cis*-diamminedichloroplatinum(II) to adenine and guanine nucleobases in the sequences d(GpApGpG):d(CpCpTpC) and d(GpGpApG):d(CpTpCpC) of A- and B-DNA. *Inorg. Chem.* **1991**, *30*, 937−942.

(8) Ling, E. C. H.; Allen, G. W.; Hambley, T. W. The preparation and characterisation of some aminesulfoxideplatinum(II) complexes. *J. Chem. Soc., Dalton Trans.* **1993**, 3705−3710.
(9) Ling, E. C. H.; Allen, G. W.; Hambley, T. W. The DNA binding of platinum(II) complex designed to bind interstrand but not intrastrand. *J. Am. Chem. Soc.* **1994**, *116*, 2673−2674.
(10) Vickery, K.; Bonin, A. M.; Fenton, R. R.; O'Mara, S.; Russell, P. J.; Webster, L. K.; Hambley, T. W. The preparation, characterization, cytotoxicity and mutagenicity of a pair of enantiomeric platinum(II) complexes with the potential to bind enantioselectively to DNA. *J. Med. Chem.* **1993**, *36*, 3663−3668.
(11) Kidani, Y.; Inagaki, K.; Iigo, M.; Hoshi, A.; Kuretani, K. Antitumor activity of 1,2-diaminocyclohexane-platinum complexes against sarcoma-180 ascites form. *J. Med. Chem.* **1978**, *21*, 1315−1318.
(12) Kidani, Y.; Noji, M.; Tashior, T. Antitumor activity of platinum-(II) complexes of 1,2-diaminocyclohexane isomers. *Gann.* **1980**, *71*, 637−643.
(13) Noji, M.; Okamato, K.; Kidani, Y.; Tashiro, T. Relation of conformation to antitumor activity of platinum(II) complexes of 1,2-cyclohexanediamine and 2-(aminomethyl)-cyclohexylamine isomers against leukemia P388. *J. Med. Chem.* **1981**, *24*, 508−515.
(14) Saburi, M.; Miyamura, K.; Morita, M.; Mizocuchi, Y.; Yoshikawa, S.; Tsuboyama, S.; Sakurai, T.; Tsuboyama, K. Stereochemical properties of copper(II) complexes of (*S*)-3-aminohexahydroazepine. Crystal and molecular structure of bromobis[(*S*)-3-aminohexahydroazepine]copper(II) perchlorate [CuBr(*S*-ahaz)$_2$]-ClO_4. *Bull. Chem. Soc. Jpn.* **1987**, *60*, 141−148.
(15) Saburi, M.; Miyamura, K.; Morita, M.; Mizocuchi, Y.; Yoshikawa, S.; Tsuboyama, S.; Sakurai, T.; Yamazaki, H.; Tsuboyama, K. Stereochemical properties of copper(II) complexes of (*RS*)-3-aminohexahydroazepine. Crystal and molecular structures of [(*R*)-3-aminohexahydroazepine][(*S*)-3-aminohexahydroazepine]-copper(II) diperchlorate, [Cu(*R*-ahaz)(*S*-ahaz)]$(ClO_4)_2$ and related complexes. *Bull. Chem. Soc. Jpn.* **1987**, *60*, 2581−2592.
(16) Comba, P.; Hambley, T. W.; Hitchman, M. A.; Stratemeier, H. Interpretation of Electronic and EPR spectra of Copper(II) Amine Complexes: A Test of the MM-AOM Method. *Inorg. Chem.* **1995**, *34*, 3903−3911.
(17) Matsunaga, K.; Fujikawa, K.; Muto, M. Novel antitumor platinum(II) complexes. Patent Application JP 87−138681, 1987.
(18) Dhara, S. C. A rapid method for the synthesis of *cis*-[$Pt(NH_3)_2$-Cl_2]. *Indian J. Chem.* **1970**, *8*, 193−194.
(19) Fanizzi, F. P.; Intini, F. P.; Maresca, L.; Natile, G.; Quaranta, R.; Coluccia, M.; De Bari, L.; Giordano, D.; Mariggio, M. A. Biological-activity of platinum complexes containing chiral centers on the nitrogen or carbon-atoms of a chelate diamine ring *Inorg. Chim. Acta* **1987**, *137*, 45−51.
(20) Price, J. H.; Williamson, A. N.; Schramm, R. F.; Wayland, B. B. Palladium(II) and platinum(II) alkyl sulfoxide complexes. Examples of sulfur-bonded, mixed sulfur- and oxygen-bonded, and totally oxygen-bonded complexes. *Inorg. Chem.* **1972**, *11*, 1280−1284.
(21) teXsan, Crystal Structure Analysis Package, Molecular Structure Corporation (1985 and 1992).
(22) Sheldrick, G. M. SHELXS-86, In *Crystallographic Computing 3*; Sheldrick, G. M., Krüger, C., Goddard, R. Eds.; Oxford Univ. Press: Oxford, 1985; pp 175−189.
(23) Cromer, D. T.; Waber, J. T. *International Tables for X-ray Crystallography*; Kynoch Press: Birmingham, 1974; Vol. 4.
(24) Ibers, J. A.; Hamilton, W. C. Dispersion corrections and crystal structure refinements. *Acta Crystallogr.* **1964**, *17*, 781−792.
(25) Creagh, D. C.; McAuley, W. J. In *International Tables for Crystallography*; Wilson, A. J. C., Ed., Kluwer Academic Publishers: Boston, 1992; Vol. C, Table 4.2.6.8, pp 219−222.
(26) Creagh, D. C.; Hubbell, J. H. In *International Tables for Crystallography*; Wilson, A. J. C., Ed.; Kluwer Academic Publishers: Boston, 1992; Vol. C, Table 4.2.4.3, pp 200−206.
(27) Johnson, C. K. ORTEP, A Thermal Ellipsoid Plotting Program; Oak Ridge National Laboratories: Oak Ridge, 1965.
(28) HyperChem, Release 2 for Windows, Autodesk, Sausalito, CA.
(29) Hambley, T. W. *MOMEC-91, Program for Strain Energy Minimisation*; Univ. of Sydney: Sydney, 1991.
(30) Page, J. D.; Husain, I.; Sancar, A.; Chaney, S. G. Effect of the diaminocyclohexane carrier ligand on platinum adduct formation, repair and lethality. *Biochemistry* **1990**, *29*, 1016−1024.
(31) Russell, P. J.; Wass, J.; Lukeis, R.; Garson, M.; Jelbart, M.; Wills, E.; Phillips, J.; Brown, J.; Carrington, N.; Vincent, P.; Raghavan, D. Characterization of cell lines derived from a multiply aneuploid human bladder transitional-cell carcinoma UCRU-BL-13. *Int. J. Cancer* **1989**, *44*, 276−285.
(32) Fujiwara, Y.; Sugimoto, Y.; Kasahara, K.; Bungo, M.; Yamakido, M.; Tew, K. D.; Saijo, N. Determinants of drug response in a cisplatin-resistant human lung cancer cell line. *Jpn. J. Cancer* **1990**, *81*, 527−535.
(33) Morikage, T.; Ogmori, T.; Nishio, K.; Fujiwara, Y.; Takeda, Y.; Saijo, N. Modulation of cisplatin sensitivity and accumulation by amphotericin B in cisplatin-resistant human lung cancer cell lines. *Cancer Res.* **1993**, *53*, 3302−3307.
(34) Mosmann, T. Rapid colorimetric assay for cellular growth and survival. Application to proliferation and cytotoxicity assays. *Immunol. Methods* **1983**, *65*, 55−64.
(35) Skehan, P.; Storeng, R.; Scudiero, D.; Monks, A.; McMahon, J.; Vistica, D.; Warren, J. T.; Bokesh, H.; Kenney, S.; Boyd, M. R. New colorimetric cytotoxicity assay for anticancer-drug screening. *J. Natl. Cancer Inst.* **1990**, *82*, 1107−1112.
(36) McKeage, M. J.; Abel, G.; Kelland, L. R.; Harrap, K. R. Mechanism of action of an orally administered platinum complex [ammine bis butyrato cyclohexylamine dichloroplatinum(IV) (JM221)] in intrinsically cisplatin-resistant human ovarian carcinoma *in vitro Br. J. Cancer* **1994**, *69*, 1−7.
(37) Lowry, O. H.; Roseburgh, N. J.; Farr, A. L.; Randall, R. J. Protein measurement with the folin phenol reagent. *J. Biol. Chem.* **1951**, *193*, 265−275.
(38) Hambley, T. W. Unpublished results.
(39) Er H. M.; Hambley, T. W. Manuscript in preparation.

JM9607966